Journal of King Saud University – Science 35 (2023) 102472

HOSTED BY

Contents lists available at ScienceDirect

Journal of King Saud University – Science

journal homepage: www.sciencedirect.com

Original article

Favorable reservoir prediction and connection model biulting of thick glutenite sediment in basin steep slope zone

Lyu Shichao [a,b,*], Song Weiqi [a]

[a] School of Geosciences, China University of Petroleum, Qingdao, Shandong 266580, China
[b] Exploration and Development Research Institute of Shengli Oilfield, Sinopec, Dongying 257012, China

ARTICLE INFO

Article history:
Received 1 July 2022
Revised 24 November 2022
Accepted 25 November 2022
Available online 1 December 2022

Keywords:
Glutenite
Nearshore subaqueous
Seismic facies
Stochastic inversion
Connection model
Lithology prediction

ABSTRACT

The glutenite deposit in the Dongying basin's dip slope zone, which is influenced by Palaeogeomorphology, has a large deposit thickness, a diverse lithology that varies rapidly in the horizon, and a difficult sand body superposition. Due to the resolution of seismic data and the vast variances across sedimentary, the connection of sand bodies cannot be represented using a simple way, and it is difficult to analyze the link regulation between water injection and oil extraction. The seismic facies of distinct glutenite sediments may be determined using well data and the properties of glutenite deposits in nearshore subaquatic settings. Several inversion techniques are used to construct the low and high-frequency component, resulting in a high-quality sand prediction result with reasonably high resolution that adheres to sedimentary laws, using seismic facies analysis as a constraint and making full use of good data. The management of sand spread and connection may be defined based on the sand prediction result, and sand body connection models of different sedimentary surfaces can be created and used to change the well water intrusion.

1. Introduction

Fault basin slope is typically characterized by a steep slope, near provenance, large ancient terrain fluctuation, and strong tectonic activities, which determine the sedimentary extensively near shore subaqueous fan, sub lacustrine fan, turbidities fan, and many other genetic types of glutenite fan bodies. For example, the nearshore underwater fan deposited during the fault depression peak period has very outstanding source-reservoir-cap relations, thus foreshadowing the formation of a Dongying Sag, southeast of Jiyang Depression, is a semi-graben basin having a steep north and sloping south, as well as a deep north and shallow south from regional expansion (Tongfei et al., 2020). The north side of the depression consists of an east–west oriented steep slope belt, an old fault stripping surface created by weathering, and denudation of the Chennan fault that regulates the valley's deposition. First, northeast and northwest faults unite to form the Chennan Fault. Later, tectonic movement, weathering, and denudation transformed it into a palaeogeographic structure with a 15°-30° fault slope, High Mountain and deep valley, and alternating gully and ridge. In the Paleogene sedimentary period, seasonal floods carried a large quantity of coarse debris along the ancient gully into the lake, and sandy glutenite fan deposits developed in the northern steep slope zone, with the nearshore underwater fan deposits primarily located in the eastern portion of the northern zone. Near-shore underwater fans have boundary faults. The nearshore underwater fan has tremendous energy and fast accumulation due to boundary fault activity. From the inner fan to the outer fan's distal end, the altering seismic facies characteristics are block phase with chaotic structure and weak amplitude (the filling phase with intermittent variable amplitude), and the phase transformation rate is faster than the continuous weak and medium amplitude-phase (Mao et al., 2021; Deng et al., 2020).

Glutenite, sandy glutenite, pebbly coarse sandstone, fine sandstone, and dark gray mudstone dominate nearshore underwater fan deposits on the northern Dongying Depression's steep slope. The gravel is composed of limestone, mud gravel, and clastic gravel, with near-source fast deposits. This type of reservoir has a deep burial depth (3000 m), diverse lithology, and fast change,

* Corresponding author at: School of Geosciences, China University of Petroleum, Qingdao, Shandong 266580, China.
E-mail address: shicl202206@163.com (L. Shichao).

Peer review under responsibility of King Saud University.

Production and hosting by Elsevier

https://doi.org/10.1016/j.jksus.2022.102472
1018-3647/

thus there are concerns with injection-production mismatch and well links. It is difficult to quantify the inter-well connectivity of effective reservoirs using typical reservoir prediction methodologies due to seismic data quality and quick phase shift inside the reservoir. The glutenite reservoir of Sha-4 member of the Yan 4 block is on the steep slope belt of the northern Dongying Sag, south of the Yan18 ancient gully. It's been under construction since 2005 when its focus moved from natural energy to water injection. Due to the small single-layer thickness of the glutenite reservoir in the study area, rapid transverse lithology change, and complex superposition relationship, water injection from adjacent wells is ineffective; therefore, connectivity characteristics between glutenite reservoirs cannot be precisely defined. From the Yan 22 block nearshore underwater fan sedimentation, the seismic reflection characteristics of different sedimentary facies belts are analyzed, and the characteristics of different seismic inversion technologies are used to fully explore the existing information about wells, optimize reservoir prediction methods, make the inversion results be in line with sedimentary facies and have high resolution, and then characterize the inversion results. The reservoir connectedness of numerous sedimentary facies belts is studied along with the injection-production law and effective reservoir prediction findings (see Fig. 1).

Glutenite, sandy glutenite, pebbly sandstone, and silty sandstone are the most common rocks. Most rocks have a subangular history, showing their proximal source and rapid accretion. The principal reservoir lithology is sandy glutenite and pebbly sandstone, and the grain size is between concentrated lithofacies; however, the physical property is outstanding, and the effective reservoir porosity is generally over 5.3 %. Sandy glutenite and pebbly sandstone have similar logging qualities, but their three-pore curves differ: glutenite has a low density and high acoustic wave, whereas silty sandstone has a high density and low acoustic wave. Based on lithology and grain size, the target layer can be classified into fan root, middle fan, and fan margin sedimentary subfacies from north to south. The inner fan is made of thick glutenite deposits, enriched gravel with grain sizes up to 15 cm and thin gray mudstone interlayers. Glutenite is poorly sorted and rounded, and most of it is sub-angular, underdeveloped in bedding, thick, and massive, with proximity to the source and rapid accumulation. The base has a scoured surface and a tiny syngenetic normal fault related to the mudstone interlayer, a residue of fault zone activity. The middle fan has glutenite, a thin layer of dark gray mudstone, and a sandy mudstone layer, and the gravel is smaller than in the inner fan. Intercalation of mudstones is prevalent in the core, suggesting frequent channel diversion, common scour structure and robust syngenetic deformation structure. The outer fan is made of dark gray mudstone interbedded with thin coarse sandstone and pebbled sandstone (Wang et al., 2022) (Fig. 2). In the longitudinal direction, rock grain size varies from course to fine from bottom to top, representing the depositional environment where water enters. Based on cycle division and isochronous face ratio, the Yan 22 block's top glutenite may be divided longitudinally into nine cyclic phases. There are apparent mudstone intervals at the interface of the two periods in most wells; therefore the sand bodies in the two periods are not connected. In a few wells, the mudstone interlayer is gone due to erosion and denudation of glutenite deposits, allowing for possible stage connections.

2. Seismic facies characteristics of the nearshore underwater fan

The extension distance of Yan 22 block glutenite is short, yet various facies zones within the offshore undersea fan exhibit distinct phase change properties during earthquakes. By classifying the seismic reflection characteristics of various sedimentary subfacies using well seismic calibration, seismic facies are then segregated. The fan-root subfacies are dominated by coarse-grained sedimentation and fast deposition, and the lithology is dominated by thick glutenite. Seismic data mostly reflect the features of

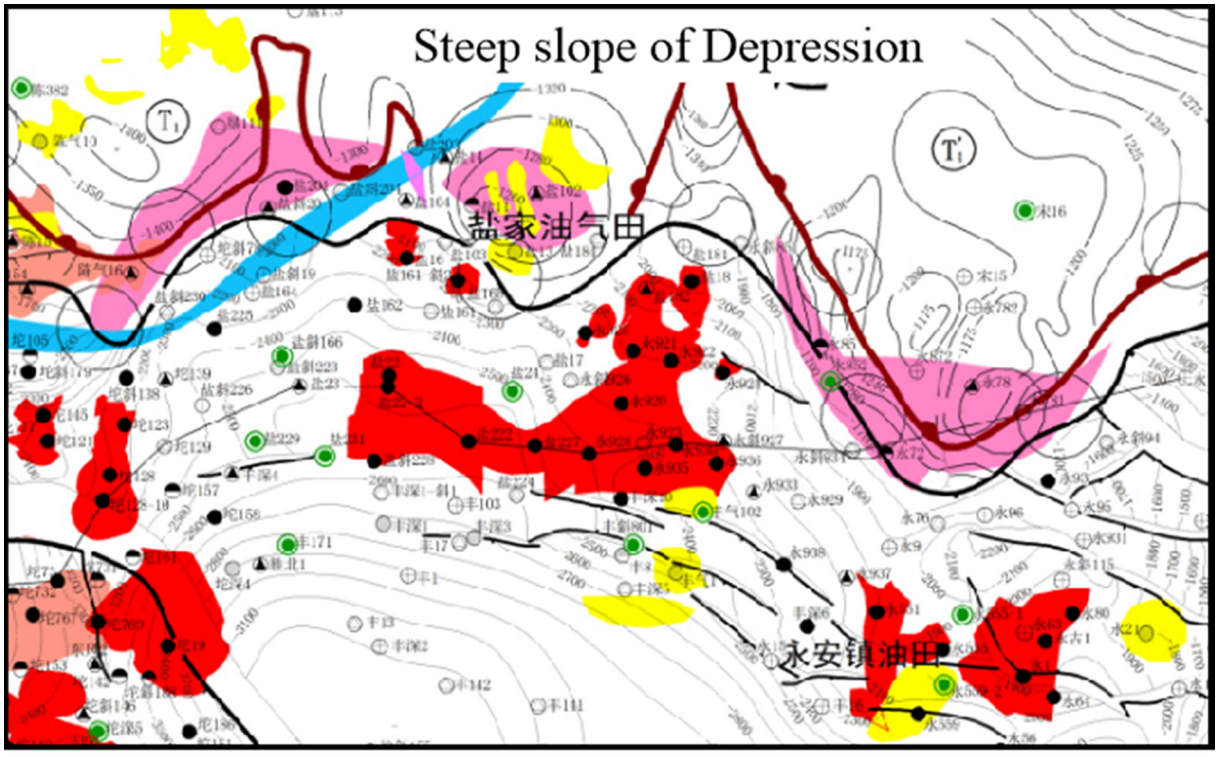

Fig. 1. Sedimentary distribution of glutenite in Yanjia Oilfield.

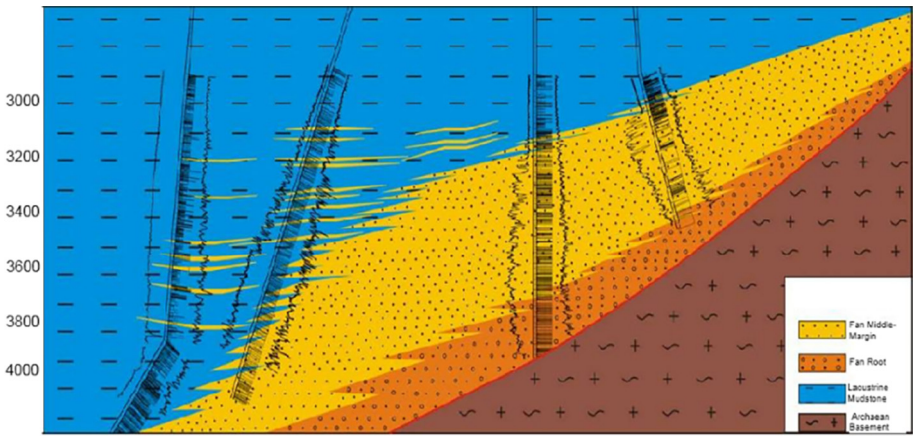

Fig. 2. Distribution diagram of sedimentary subfacies of Yanjia nearshore underwater fan.

chaotic reflection due to the enormous sedimentary thickness and lack of visibility of the sedimentary interface. It is a good facies belt for reservoirs, and the effective thickness of the superposition is considerable. In addition, it exhibits sequence and cycle features in sedimentation and stratification in seismic reflection, although its continuity is limited. On the end of the fan, the subfacies consist mostly of fine sandstone, while mudstone is moderately developed. Sandstone and fine sandstone may be reasonably advantageous reservoirs, but the thickness of a single layer is limited, and the seismic reflection characteristics are comparable to those of glutenite sedimentary lacustrine mudstone in the south, with strong continuity. There is often an encompassing surface reflection between the fan end and lacustrine facies mudstone that may be used as an indication to differentiate the distinct sedimentation (Liu 2022, Zhou et al., 2020). In general, there is a gradual transition between the three subphases, and the transitional interface between them is not readily apparent (Fig. 3).

In conjunction with the seismic reflection characteristics of various subfacies, the glutenite reflection is split into three seismic facies, and their distinct seismic reflection characteristics are then examined (Table 1). In general, the three subfacies have distinct amplitude, frequency, and waveform properties. The seismic body attributes are retrieved based on these characteristics to indicate the variations in the glutenite facies zone and the changing characteristics between glutenite and lacustrine deposits (Fig. 4):

(1) Total energy attribute: the total energy attribute can detect amplitude anomaly or sequence features, efficiently identify lithologic or gas-bearing sandstone changes, and then differentiate conformable sediment, moundy sediment, etc.

(2) Dominant frequency attribute: the dominant frequency attribute reflects the transverse variation characteristics of seismic dominant frequency caused by gas saturation, fault system change, lithology change, etc., and can reveal the hidden frequency trend caused by strata, lithology, or tuning change.

(3) Chaos attribute: The Chaos attribute is primarily used to reflect the discontinuity of seismic reflection information and the chaotic degree of signal, which may disclose the variations in the features of the seismic reflection signal generated by lithology or sedimentary characteristics. Due to the varied sedimentary and lithofacies features in different sedimentary facies zones, the chaotic attribute value for the nearshore underwater fan sedimentation in the research region falls progressively from fan root to fan body edge.

(4) Texture attributes highlight the discontinuity characteristics of seismic data caused by faults, fractures, and sedimentation by constructing seismic texture units and gray co-occurrence matrices and reflecting the comprehensive information of seismic data in terms of direction, interval, and variation amplitude (Li et al., 2022).

Under the influence of sedimentary facies and lithofacies features, the texture properties from the fan root to the fan end and

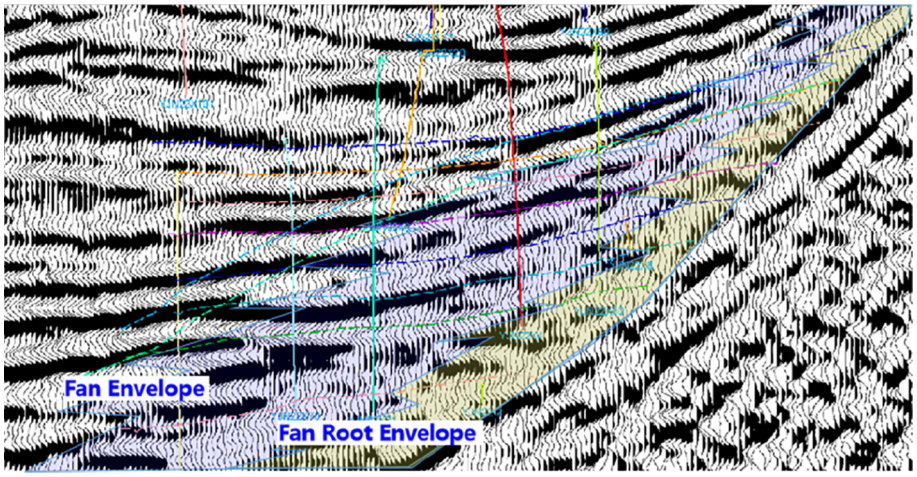

Fig. 3. North-South seismic section of Yan 22 block glutenite.

Table 1
Seismic facies classification of Yan 22 block glutenite.

Subfacies	Frequency	Amplitude	Waveform	Reflection Form
Fan Root	4–28 Hz	Wead	Chaos	High positive curvature across the source direction
Fan Middl	11–22 Hz	Middle	Low Continuity	High positive curvature across the source direction
Fan Margin (include mudstone)	9–25 Hz	High	High Continiuty	Gentle

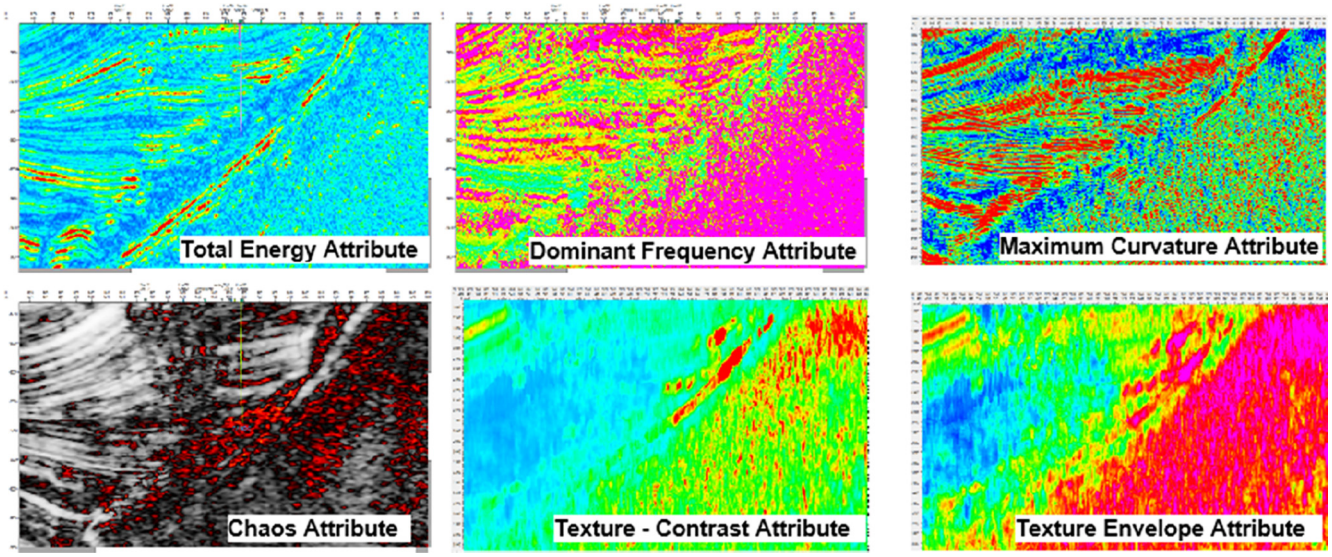

Fig. 4. Seismic property profile of glutenite.

from the sedimentary core to the two wings of the fan body decrease progressively, and the variation characteristics resemble the chaotic attribute.

(5) Maximum curvature attribute: nearshore underwater fan sedimentary formation is heavily impacted by ancient landforms, the lateral variation is greater, and fan body features are evident, thus the core and sides of the fan have distinct morphological variations. In general, the positive curvature value in the center of the deposition is the greatest, and on both sides of the fan body, the deposition vanishes, or the negative curvature at the intersection of the two fans is the greatest, while that on both wings of the fan and front-end is less.

3. Seismic prediction of glutenite reservoir

3.1. Low-frequency trend establishment

In a traditional inversion, the low-frequency model primarily uses the good interpolation approach, which is often suitable when there are numerous equally dispersed wells or when geological and tectonic changes are not extreme. Due to the characteristics of rapid phase transformation in glutenite, however, the wings of the fan body decrease rapidly, and old wells are frequently fewer and more concentrated in the deposition center area, so the changing trend of the glutenite sand body toward the wings and away from the provenance cannot be accurately reflected by the good point interpolation method (Babikir et al., 2022; Guan et al., 2022; Owusu and Raef, 2022). In certain instances, there may be a few wells in the lake basin direction that are located distant from the fan body, making them susceptible to the "bull's eye" phenomena during the creation of the low-frequency model, so impacting the subsequent inversion effect.

Based on the seismic facies analysis and dominant attribute extraction under the sedimentary law of the nearshore undersea fan and the related seismic facies characteristics, an acceptable low-frequency model is developed. There is an abundance of drilling data in the study area, and the main frequency, amplitude, energy, degree of chaos, and texture attributes can reflect the characteristics of different facies of glutenite fan body and lake facies mudstone sedimentation from multiple perspectives; therefore, the use of these properties based on neural network learning method to establish the mapping relationship between seismic attributes and well point wave impedance, and then predict the wav. To remove the medium and high-frequency information contained in the seismic attributes and wave impedance curves, the seismic attributes and wave impedance curves must be filtered before neural network fitting so that only low-frequency information can participate in the fitting and prediction process.

The low-frequency model developed by attribute restriction has a more acceptable variation trend in the fewer-well controlling regions, particularly in the perimeter of glutenite and the sides of the fan body, which is more compatible with the sedimentary law than the traditional model (Fig. 5). In general, the low-frequency models derived by the two techniques have the same trend, and the wave impedance values decline progressively from the fan root near the base to the direction of the lake basin, with the two wings exhibiting a lower tendency. On the east side of the Yan 22 block fan body, for instance, since it shares a border with another set of glutenite (Yan 222 block fan), the region touched by the two fan bodies is impacted by lateral migration of glutenite sedimentation, which is truly glutenite interbedding sedimentation. In the meanwhile, lithology should correlate to high levels of reflection impedance. If the east well data is not used, or if there is no east well, the standard low-frequency model has low impedance at this location (Fig. 5a). In this instance, the attribute constraint approach is used to present relatively high values in the east, allowing the impedance values in this region to adhere

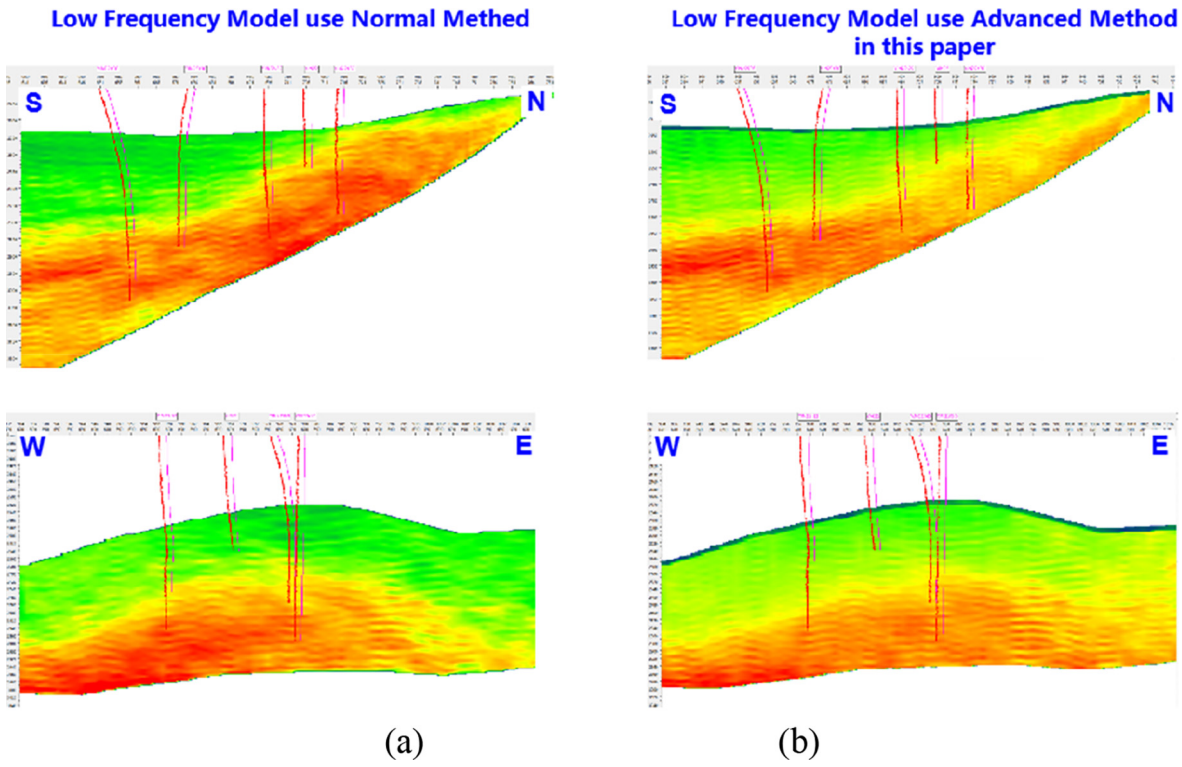

Fig. 5. Comparison section of low-frequency model effect.

to the real geological variation features and be confirmed by previously drilled wells.

3.2. Sparse pulse inversion

According to the seismic resolution of the studied region, the thickness of the seismically recognizable geological body is about 35 m, which is significantly more than the thickness of a single sand body. Nevertheless, from the standpoint of sedimentary law, this thickness may correspond to the major channel of glutenite sedimentation, i.e. a sand group having many effective reservoirs. Utilizing sparse pulse inversion, the distribution of dominating sand formations may be accurately characterized. Based on a low-frequency model that complies with sedimentary law and is governed by dominant characteristics, sparse pulse inversion is used to forecast the distribution framework of dominant sand formations.

According to the findings of the inversion, the fan root location is characterized by a high impedance, and there are no blatant indications of channel migration. In these places with high impedance, effective reservoirs are not constructed due to the findings of the physical investigation of the rocks. In the center fan region, there is a distinct difference in wave impedance, suggesting that there is a dominating glutenite period area that may be defined using the impedance values of rock physics analysis. At the fan end, the features of the dominating reservoir are evident. In comparison to the mudstone barrier, the effective reservoir has comparatively high resistance (Fig. 6).

Due to the complex sedimentary characteristics of the offshore underwater fan and the thin effective reservoirs, sparse pulse inversion can reflect favorable sand group distribution; however, higher resolution prediction results are necessary to analyze the distribution of effective reservoirs and the connectivity relationship.

3.3. Stochastic constrained inversion

Affected by the seismic resolution, sparse pulse inversion can reflect the distribution of dominant sand groups and describe the glutenite reservoir framework, but it cannot distinguish the single sand body within the sand group and therefore cannot be used to describe the contact relationship between sand bodies. To better characterize the glutenite reservoir, the stochastic-constrained inversion approach is utilized. Combining the geostatistics approach with the inversion principle and integrating the wave impedance data volume converted by well point lithologic data and seismic data (Yang et al., 2022; Liu et al., 2022; Mattia and Alessandro, 2020), stochastic seismic inversion creates a 3D geological model. Due to the unpredictability of geology, the vertical resolution of seismic data may be considerably increased under the constraints of good data, as shown by the stochastic simulation result for reservoir prediction. Therefore, the heterogeneity of the reservoir can be accurately reflected in three-dimensional space, and the multi-solution of reservoir description by well data statistical relationship is reduced, which facilitates the prediction of the thin reservoir with a small distribution scale and rapid transverse transformation (Rashad et al., 2022; Zhang et al., 2022; Wang et al., 2022). The impedance body derived from sparse pulse inversion is employed as the starting model for seismic random inversion for suitable reservoirs in the research region. Then, depending on the seismic resolution, numerous good data from the region are added to the high-frequency information.

Given the features of fast lateral variation of nearshore undersea fan deposition, it is incorrect to pick the region-wide uniform prior probability for stochastic inversion. The spatial probability density field of the prior probability density function is first determined. As the statistical findings of well-point data are discrete, continuous ergodic functions cannot be derived from good information; thus, the spatial probability density must be computed using the data volume acquired from wave impedance inversion.

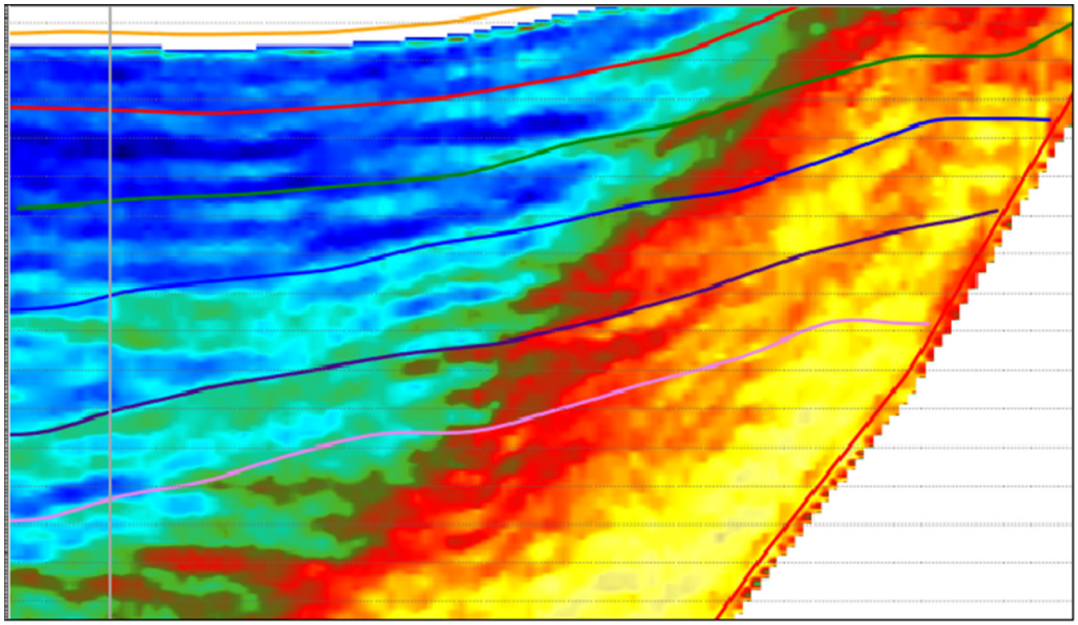

Fig. 6. Sparse pulse inversion profile.

Establishing the field function by statistical analysis of well points and construction of the field function of the impedance-probability density function. Using the statistics of well point information, it is possible to assume that in the time window of the corresponding seismic resolution, the high-frequency impedance of the good point corresponding to a specific average wave impedance follows a Gaussian distribution, and the three-dimensional probability density function of the point is subsequently constructed by regression analysis as the prior probability density function:

Where x, y, and z are the coordinates of a specific point in space, Imp is the p-wave impedance value; σ is the scale function, and μ is the position function, which requires fitting and calculating the data values in the impedance volume obtained by the coefficient pulse inversion in the calculation window. In general, the value of μ is near to the average wave impedance in the time frame, and the average value may be used directly as the value in a zone with few wells or no wells. When the lithologic properties of a particular target region are understood, the impedance value range is essentially defined. To protect the integrity of inversion data, each statistical point's probability density function must satisfy the following conditions:

$$\int_{Imp_{min}}^{Imp_{max}} P(x,y,z,Imp)dImp > 0.99 \int_{Imp_{min}}^{Imp_{max}} P(x,y,z,Imp)dImp > 0.99 \quad (1)$$

Imp_{min} Where Imp_{min} and $Imp_{max}Imp_{max}$ are the lowest and maximum wave impedance values of the lithology in the applicable work area. If this requirement is not satisfied, it is required to examine the sample sites' logging curves and lithology interpretation for abnormalities.

The following describes the relationship between seismic data and the geological model:

$$d = f(m) + ed = f(m) + e \quad (2)$$

where d is the seismic record, f(m) is the forward operator, m is the model parameter, the starting model may be derived randomly from the prior probability density field, and e is random noise.

The posterior probability distribution for the link between model parameters and observed data may be determined using Bayes' principle.

$$p(m|d) = \frac{p(d|m)p(m)}{p(d)} p(m|d) = \frac{p(d|m)p(m)}{p(d)} \quad (3)$$

where p (m) is the prior probability density, which varies spatially for nearshore underwater fan deposition, and whose distribution properties may be derived from Equation (3). P(d) is the constant that has been normalized; p(d|m) is the likelihood function, which measures the degree of reflection between model and data and is often written as a multivariate Gaussian distribution:

$$p(d|m) = \frac{1}{\sqrt{(2\pi)|C_d|}} e^{-\frac{(d-d(m))^T C_d^{-1}(d-d(m))}{2}} p(d|m) = \frac{1}{\sqrt{(2\pi)|C_d|}} e^{-\frac{(d-d(m))^T C_d^{-1}(d-d(m))}{2}} \quad (4)$$

where C_dC_d is the observed data's covariance matrix. When the model is compatible with the observed data, p(d|m)p(d|m) has the same distribution as noise.

In the case of creating prior information and likelihood function based on sedimentary properties, the Bayesian inversion issue is handled using the Markov Chain Monte Carlo (MCMC) technique, and high-precision inversion results are achieved (Fig. 7). The resolution of the findings of inversion is much greater than that of sparse pulse inversion. In the meanwhile, since the prior probability distribution is compatible with sedimentary law, the inversion findings are also consistent with the sedimentary facies characteristics, which may describe the transverse variation features of the nearshore underwater fan sedimentation.

4. Analysis of development laws of connecting sand bodies

Based on the prediction results of the glutenite reservoir and the existing injection-production correspondence analysis, the connectivity characteristics of different facies zones of the glutenite reservoir are described and analyzed, and the sand body connectivity models of different facies zones are subsequently developed. The superposition and contact relationships of glute-

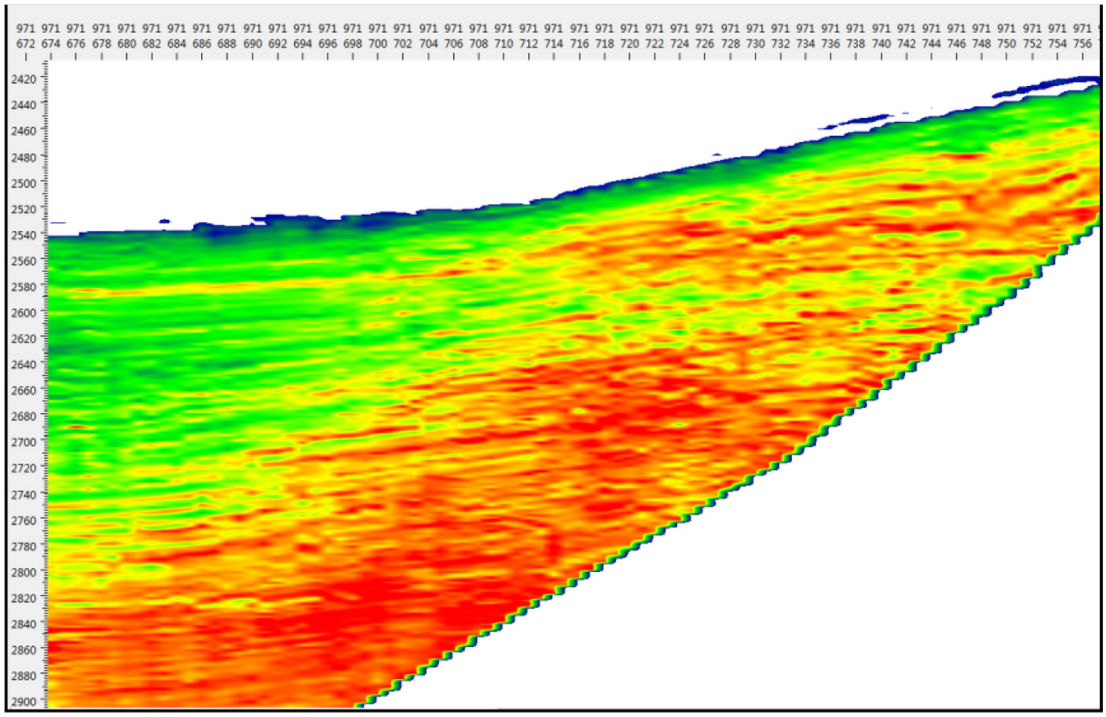

Fig. 7. Stochastic inversion profile of Yan 22 block.

nite sand bodies in several facies zones exhibit distinct properties (Table 2):

(1) The sand body of fan end subfacies has long extension and good continuity

According to fan-end finishing, the sedimentary grain size is fine, and there are several non-reservoirs such as mudstone and siltstone, with medium and fine sandstone constituting the majority of reservoirs. The single sand body has a long extension distance, a wide horizontal reservoir continuity, and excellent physical qualities. Additionally, there is minimal interaction between various sand bodies, so the injection-production pattern design is appropriate.

(2) The sand body of fan subfacies is partially superimposed and connected

In the middle glutenite fan region, there are several lithologic kinds, including glutenite with poor sorting and low physical qualities and siltstone with tiny grain size, although pebbly sandstones are comparatively developed as an efficient reservoir. There is a

Table 2
Connectivity model of nearshore underwater fan sand body.

Facies types	Reservoir prediction profile	connectivity model of dominant sand body	Main lithology of facies zone
Fan end	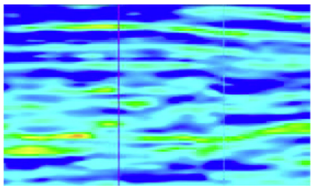	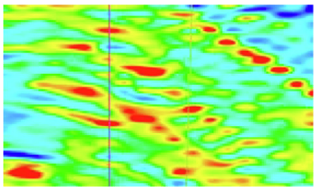	Medium-fine sandstone Siltstone Mudstone
Middle fan	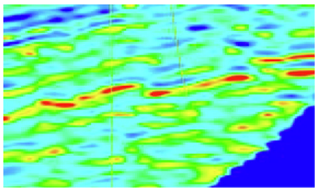	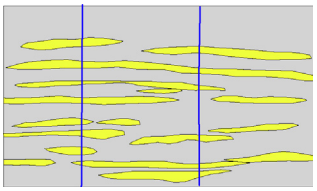	glutenite Conglomeratic sandstone Siltstone Mudstone
Fan root	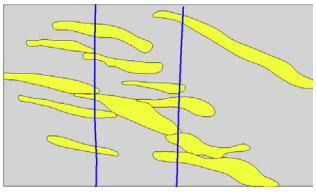	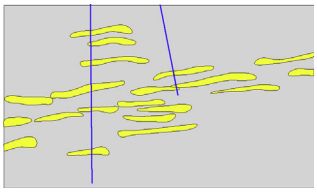	glutenite Conglomeratic sandstone

complex relationship between reservoir connectivity and injection-production correspondence due to the influence of lateral migration and deposition of sand bodies on the distribution of sand bodies. Furthermore, the superimposed relationship changes significantly, creating a complex relationship between reservoir connectivity and injection-production correspondence. Overall, the sandstone is strongly linked from north to south and weakly connected from east to west because of the origination orientation. When the sandstone is horizontally stacked, there are additional injection-production linkages in separate vertical provenance orientations.

(3) The effective sand body of fan root subfacies is small in size and poor in connectivity

Subfacies glutenite form well in the fan root, but overall sorting is poor. Pebbly sandstone and sandy glutenite are relatively dispersed as effective reservoirs, and after analyzing the injection-production relationship between wells, it is believed that the sand body connectivity of fan roots is poor. Well-drilling reveals thick reserves in this location, which is paradoxical. In conjunction with the seismic inversion results, it is evident that although the two adjacent wells have well-developed reservoirs near the borehole, the malleability of sand bodies is poor, primarily consisting of small, thin sand bodies, and the connectivity of sand bodies between adjacent wells is poor.

5. Conclusions

In Tibet's high-altitude regions, the climate is complicated. These qualities make it challenging to regulate temperature and prevent cracks in bulk concrete. Future estimates of prospective reservoirs will be based on geological structure characteristics, logging interpretation results, oil test results, and other factors. In parallel, we will keep improving the algorithm to improve the precision of predicting suitable reservoirs using machine learning.

Declaration of Competing Interest

The authors declare that they have no known competing financial interests or personal relationships that could have appeared to influence the work reported in this paper.

Acknowledgment

The authors are thankful to the higher authorities for the facilities provided.

Statements and Declarations

The author declares that no conflict of interest is associated with this study.

Authors' contribution

This study was done by the authors named in this article, and the authors accept all liabilities resulting from claims which relate to this article and its contents.

Availability of data and materials

The data used to support the findings of this study are available from the corresponding author upon request.

Funding

No funding was received for this study.

References

Babikir, I., Elsaadany, M., Sajid, M., Laudon, C., 2022. Evaluation of principal component analysis for reducing seismic attributes dimensions: Implication for supervised seismic facies classification of a fluvial reservoir from the Malay Basin, offshore Malaysia. J. Pet. Sci. Eng. 217, 110911.

Deng, J., Xia, S., Liu, J., Wu, P., Du, X., Chang, Y., Gao, L., Zheng, X., Ma, J., 2020. Sequence architecture and depositional evolution of Dongying Formation in steep slope zone of northern Liaodong Bay and its responses to tectonism. Geol. J. 55 (7), 5251–5274.

Guan, X., Meng, Q., Jiang, C., Chen, X., She, R., Sun, L., 2022. Application of facies controlled prestack inversion technology in prediction of deep tight gas in continental faulted basin. Geofluids 2022.

Li, N., Zhang, J., Luan, X., 2022. Predicting thin sand beds and subtle lithologic traps in the shahejie formation of the Chezhen sag by joint investigation of seismic facies using 3D Seismic data. Arab. J. Sci. Eng. 47 (6), 7407–7418.

Liu, W., Du, W., Guo, Y., Li, D., 2022. Lithology prediction method of the coal-bearing reservoir based on stochastic seismic inversion and Bayesian classification: a case study on Ordos Basin. J. Geophys. Eng. 19 (3), 494–510.

Liu, S., 2022, May. Study on Reservoir Diversity Controlled by Multiple Factors: An example from Liushagangzu 3rd member of Northern Steep SlopeZone in Weixinan Depression, Beibuwan Basin, South China Sea. In EGU General Assembly Conference Abstracts (pp. EGU22-4941).

Mao, S., Hao, X., Gong, J., Zhang, P., Qiu, Y. and Wang, W., 2021, July. Hydrocarbon accumulation characteristics and model of deep-seated glutenite on steep slope zone of fault basin: a case study of the E2s4 Member in Yanjia area, Dongying Sag. In: IOP Conference Series: Earth and Environmental Science, vol. 804, No. 2, IOP Publishing, p. 022039.

Mattia, A., Alessandro, S., 2020. Markov chain Monte Carlo algorithms for target-oriented and interval-oriented amplitude versus angle inversions with non-parametric priors and non-linear forward modelings. Geophys. Prospect., 735–760

Owusu, P.A., Raef, A., 2022. Machine learning in reservoir characterization: Coupling data resolution-enhancement with hierarchical analysis of 3D seismic attributes for seismic facies classification. In: Second International Meeting for Applied Geoscience & Energy. Society of Exploration Geophysicists and American Association of Petroleum Geologists, pp. 1344–1348.

Rashad, O., El-Barkooky, A.N., El-Araby, A., El-Tonbary, M., 2022. Deterministic and stochastic seismic inversion techniques towards a better prediction for the reservoir distribution in NEAG-2 Field, north Western Desert. Egypt. Egypt. J. Petrol. 31 (1), 15–23.

Tongfei, H., Diqiu, Z., Yuejun, L., Aixiang, L., Dingsheng, C., Weili, K., Beiwei, L., Yanqi, W., Hong, L., 2020. Characteristics of transfer structures and hydrocarbon accumulation control in the western steep slope zone of the Fula sag, Muglad Basin, Sudan. China Petrol. Explorat. 25 (4), 105.

Wang, Z., Chen, T., Hu, X., Wang, L., Yin, Y., 2022a. A multi-point geostatistical seismic inversion method Based on local probability updating of Lithofacies. Energies 15 (1), 299.

Wang, W., Pijl, A., Tarolli, P., 2022b. Future climate-zone shifts are threatening steep-slope agriculture. Nature Food 3 (3), 193–196.

Yang, X., Wang, F., Zhang, M., 2022. Facies-controlled inversion in the prediction of volcanic rock and surrounding reservoir with near offset stack seismic: a case study in No. 2 structure of Nanpu sag. Prog. Geophys. 37 (4), 1640–1649.

Zhang, X., Fu, J., Hou, F., Zheng, X., Zhang, Y., Wang, R., Li, W., Zhai, C., Wang, W., He, R., Liu, J., 2022. Sand-mudstone modeling of fluvial fan sedimentary facies: a case study of Shanxi Formation reservoir in Ordos Basin. J. Pet. Explor. Prod. Technol., 1–14

Zhou, S., Yongfu, L., Jianfa, H., Haining, L., Fengying, Y., Yuzhe, C., 2020. Application of ultra-deep sandstone reservoir prediction technology under controlled seismic facies in Yudong block of Tabei Uplift, Tarim Basin, China. J. Natural Gas Geoence 5, 157–167.